

Charge separation effects in magnetized electron-ion plasma expansion into a vacuum

Kazumi Nishimura, Edison Liang^{a)}, and S. Peter Gary

Los Alamos National Laboratory, Los Alamos, NM 87545

^{a)}*Rice University, Houston, TX 77005-1892*

(Dated: October 19, 2018)

Charge separation effects in the expansion of magnetized relativistic electron-ion plasmas into a vacuum are examined using 2-1/2-dimensional particle-in-cell plasma simulations. The electrostatic field at the plasma surface decelerates electrons and accelerates ions. A fraction of the surface electrons are trapped and accelerated by the pondermotive force of the propagating electromagnetic pulse, a mechanism we call the DRPA (diamagnetic relativistic pulse accelerator). This charge separation is enhanced as the initial plasma temperature is decreased. The overall energy gain of the plasma particles through the expansion strongly depends on the initial plasma temperature. Moreover, the electrons become relatively less energized and the ions more energized as the plasma temperature decreases.

PACS numbers:

Several kinds of plasma expansions have been investigated over the past few decades. A model of free plasma expansion into a vacuum is interesting for studies related to experiments of ion jets[1, 2]. Structures and instabilities of plasmas expanding into a vacuum which contains a uniform ambient magnetic field have also been examined by theoretical and numerical methods. Those studies are relevant to laser-plasma experiments[3, 4] and space plasma phenomena[5, 6, 7]. Also plasma injection into a magnetic field has been theoretically investigated[8].

Recently, Liang *et al.*[9, 10] have studied a new type of plasma expansion, in which a magnetized relativistic plasma freely expands into a vacuum with no external magnetic field. This model of expansions potentially can be applied to a variety of astrophysical phenomena, such as gamma-ray bursts[10] or astrophysical jets. When relativistic plasmas which contain a strong transverse magnetic field are suddenly released, an EM pulse forms and begins to propagate into the vacuum. Simultaneously, a portion of the surface plasma is trapped and accelerated by the EM pulse via the pondermotive force. Through the expansion, the field energy of the EM pulse is converted into the directed kinetic energy of the surface particles. This new mechanism of plasma acceleration is called the diamagnetic relativistic pulse accelerator (DRPA) [9].

Electrons and ions behave differently in the expansion process. Because of their much smaller mass, the surface electrons soon outrun the ions and charge separation occurs. In this Letter, using the results of plasma full particle simulations, we discuss charge separation effects on plasma energization in the relativistic magnetized plasma expansion into a vacuum.

In our particle simulation code[11], we use a two-and-a-half-dimensional explicit simulation scheme based on the particle-in-cell method for time advancing of plasma particles. The grid separations are uniform, $\Delta x = \Delta z = \lambda_e$, where λ_e is the electron inertial length defined by c/ω_{pe} (c is the speed of light and the electron plasma frequency is $\omega_{pe} = \sqrt{e^2 n_0 / \epsilon_0 m_e}$; e is elementary charge,

n_0 is the initial electron density, and ϵ_0 is the dielectric constant of vacuum). The ratio of the electron Larmor frequency to the electron plasma frequency Ω_e/ω_{pe} (where $\Omega_e = eB_0/m_e$; B_0 is the background magnetic field) is set equal to 10 in these simulations. The ion-electron mass ratio is $m_i/m_e = 100$ and the charge ratio is $q_i/e = 1$. The simulation domain on the $x-z$ plane is $-L_x/2 \leq x \leq L_x/2$ and $-L_z/2 \leq z \leq L_z/2$. To prevent large violations of Gauss's law due to numerical noise, Marder's method for the electric field correction[12] is adopted at every time step in the code.

We use a doubly periodic system in x and z directions, and the system length is $L_x = 240\Delta x = 2400c/\Omega_e$ and $L_z = 120\Delta z = 1200c/\Omega_e$. Initially, the electron (ion) distributions are assumed to be a relativistic (non-relativistic) Maxwellian respectively with spatially uniform temperature. The spatial distribution of the initial plasma has a slab form with the lengths $6\Delta x \times 120\Delta z$, and the plasma slab is located in the center of the system. The background magnetic field $\mathbf{B}_0 = (0, B_0, 0)$ initially exists only inside the plasma. Since the system length in the x direction is enough large, no plasma particles and waves can cross the x boundaries during this calculations (until $t\Omega_e = 1000$).

We describe here the results of two simulations; one with initial temperatures of $k_B T_e = k_B T_i = 5MeV$ and one with initial temperatures of $k_B T_e = k_B T_i = 100keV$. The qualitative evolution of the $5MeV$ temperature case is illustrated in Figure 5 of Ref.[9]. A pulse of fast electrons moves rapidly away from the ions in the x -direction, carrying an imbedded electromagnetic pulse ($B_y > 0$, $E_z < 0$) with them which permits them to $E \times B$ drift. Behind this pulse the B_y and E_z are relatively weak, and the expanding ions lag well behind the electron pulse. This charge separation leads to an E_x in the region between the electron pulse and the fastest ions.

Spatial profiles of the EM field and the plasma density at $t\Omega_e = 600$ are displayed in Figure 1 for the $100keV$ temperature case. In Fig. 1(a), the EM pulse is propagating in the positive x direction. The electrostatic field E_x

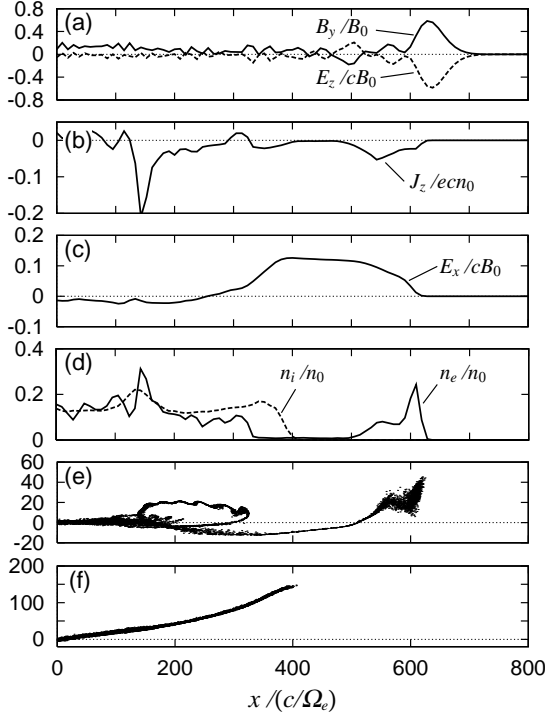


FIG. 1: Simulation results for $k_B T = 100 \text{ keV}$ plasma at $t\Omega_e = 600$. (a) Electromagnetic field (E_z and B_y), (b) current density (J_z), (c) electrostatic field (E_x), and (d) electron and ion density (n_e and n_i) as functions of x . All of the quantities are obtained at $z = 0$. Phase plots $p_x/m_e c - x$ for (e) electrons and (f) ions. These profiles should be compared with those of the $k_B T = 5 \text{ MeV}$ case in Ref.[8].

shown in Fig. 1(c) is generated by the charge separation between electrons and ions. As shown in Fig. 1(d), electrons are distributed spatially more extensively than ions because of the larger mobility of electrons. In the case of electron-positron expansion [9], there is no difference in the density distributions of electrons and positrons. Consequently, both electrons and positrons are equally energized by the DRPA. But in the present electron-ion case, only electrons can follow and get energized by the EM pulse, while the ions are accelerated in a secondary manner by the charge-separation electric field.

Phase plots $p_x/m_e c - x$ of (e) electrons and (f) ions at $t\Omega_e = 600$ in the 100 keV temperature case are also shown in Fig. 1. In Fig. 1(e), electrons are decelerated in the region $300 < x/(c/\Omega_e) < 600$, where the electric field E_x exists. The surface electrons in the vicinity of $x \simeq 600c/\Omega_e$ are strongly energized by the EM pulse. Since some of the expanding electrons are reflected at the potential wall of the electrostatic field at $x \simeq 300c/\Omega_e$, a loop structure in phase space can be seen. On the contrary, the front ions in this region are accelerated by E_x and the averaged kinetic energy of the front ions tends to increase with time. The front ions are not affected by the DRPA since the ions cannot follow the EM pulse. Hence, we obtain an interesting result regarding particle

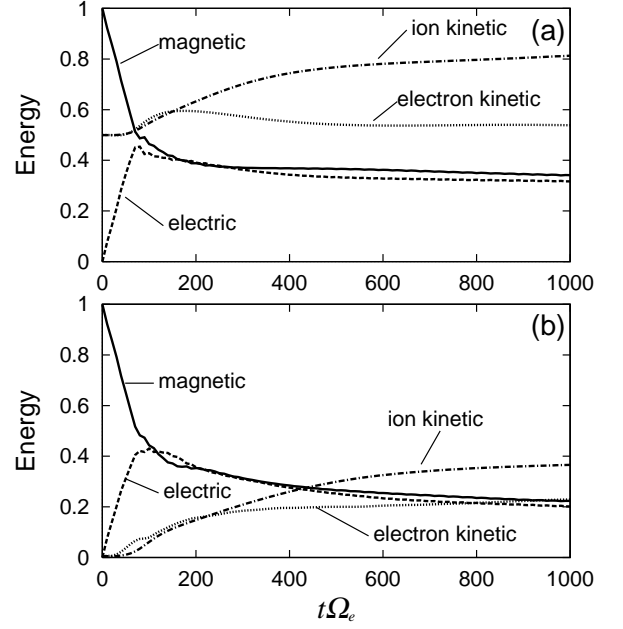


FIG. 2: System-integrated energy in the magnetic field, electric field, electrons, and ions for (a) $k_B T = 5 \text{ MeV}$ and (b) $k_B T = 100 \text{ keV}$ plasmas. Each energy is normalized by the initial magnetic field energy in each figure.

energization in the electron-ion plasma expansion: the surface electrons expanding in phase with the EM pulse are accelerated by the DRPA, but a portion of the front electrons are also decelerated by the electrostatic field E_x caused by the charge separation, while the front ions are always accelerated by E_x . Here, we showed only the 100 keV temperature case in Fig. 1. See Ref.[9] for the profiles of the 5 MeV case.

Temporal evolutions of each energy component through the expansion are shown in Figure 2 for two cases with (a) $k_B T_e = k_B T_i = 5 \text{ MeV}$ and (b) $k_B T_e = k_B T_i = 100 \text{ keV}$. Note that in case (a) the initial plasma β (=plasma pressure/magnetic pressure) = 0.216 while in case (b) $\beta = 0.02$, so the plasma is strongly magnetic-dominated. During $0 < t\Omega_e < 80$, roughly corresponding to the light crossing time of the initial plasma slab, the system evolves from the initial magnetostatic configuration into two counter-propagating EM pulses loaded with plasma. In this early phase, the magnetic energy decreases and the electric energy increases until the two are almost equal. After $t\Omega_e \simeq 80$, the field energy decays and is converted into the directed kinetic energy of plasma particles. In Figs. 2(a) and (b), we observe the monotonic increase of the total kinetic energy of the ions at all times. The total electron energy, however, decreases from $t\Omega_e = 80$ to 400 in the $k_B T = 5 \text{ MeV}$ case, and hardly changes after $t\Omega_e = 400$ in Fig. 2(a). Even for the 100 keV case of Fig. 2(b), though the total electron energy increases monotonically, we see that the rate of increase of electron energy is much smaller than that

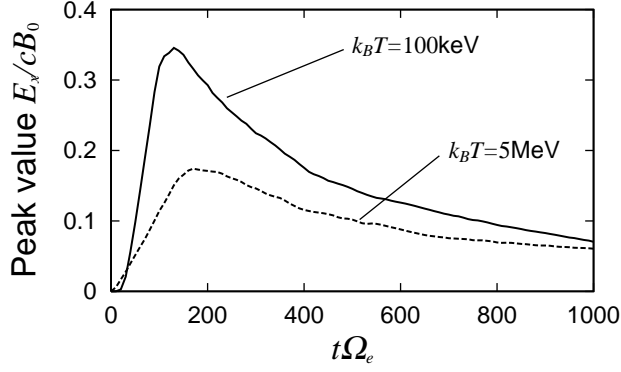


FIG. 3: Temporal evolution of peak value of electrostatic field E_x . Comparison between different temperature plasmas.

of the ion energy. In addition, the decrease of the total electron kinetic energy in Fig. 2(a) is mainly caused by the deceleration due to the electrostatic field E_x (we described the details in Figure 1). The same thing happens also in Fig. 2(b). But because the initial thermal energy of electrons is less than the directed kinetic energy given by the DRPA, the overall kinetic energy of electrons increases monotonically for the 100 keV plasma.

In Figure 3, the peak value of E_x for different initial temperatures are shown as a function of time. The electrostatic field E_x peaks in the vicinity of the ion front. At the early phase of the plasma expansion ($t\Omega_e \simeq 180$ in Fig. 3), the field E_x is formed by the charge separation. After that period, the density difference between electrons and ions is gradually reduced by ion acceleration and electron deceleration due to E_x . As a result of this, the field E_x becomes weaker. A plasma tends to be spatially broader as its temperature becomes higher. Accordingly, the higher the plasma temperature, the smaller the density difference between electron and ion becomes. That is why the peak value of E_x in the case of the 100 keV temperature plasma tends to be larger than that of the 5 MeV temperature plasma in Fig. 3.

Let us evaluate quantitatively how the field E_x influences particle energization. Fig. 4 displays the momentum distribution of the front electrons at three different times for initial plasma temperatures of (a) $k_B T = 5 \text{ MeV}$ and (b) $k_B T = 100 \text{ keV}$. The front electrons are accelerated by the DRPA and simultaneously decelerated by the electrostatic field as the expansion proceeds. The energy gain of these electrons seems to be positive and the kinetic energy continues to increase as time elapses, as shown in Fig. 4.

This means that the acceleration process dominates the deceleration process overall for the front electrons. Figs. 4(a) and 4(b) show that the electron energy gain depends on the initial plasma temperature. The electric field induced by charge separation tends to be smaller when the plasma temperature is higher. Thus, the front electrons are more strongly decelerated in the low temperature case, and the energy gain of the electrons be-

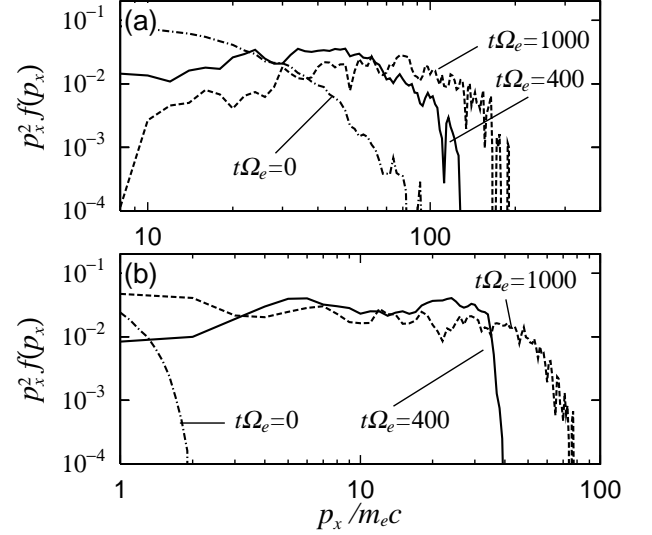


FIG. 4: Momentum distributions of electrons in the expansion front $p_x/m_e c - x$ for (a) $k_B T = 5 \text{ MeV}$ and (b) $k_B T = 100 \text{ keV}$ plasmas at $t\Omega_e = 0, 400$, and 1000 .

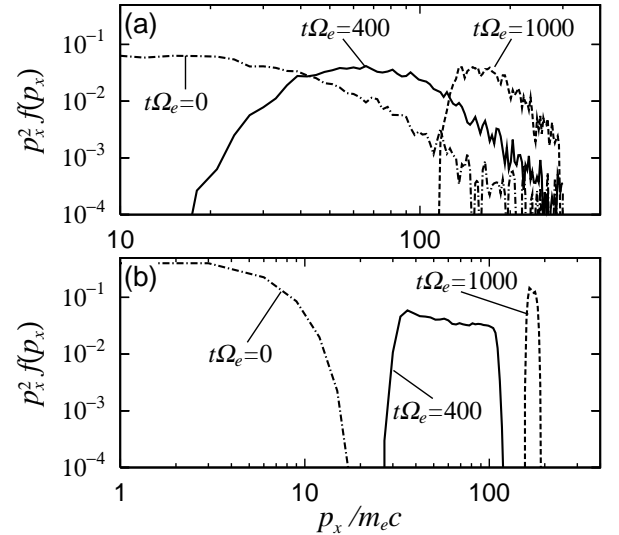


FIG. 5: Momentum distributions of ions in the expansion front $p_x/m_e c - x$ for (a) $k_B T = 5 \text{ MeV}$ and (b) $k_B T = 100 \text{ keV}$ plasmas at $t\Omega_e = 0, 400$, and 1000 .

comes large when the temperature is high.

Figure 5 displays the momentum distribution of the ions in the expansion front for (a) $k_B T = 5 \text{ MeV}$ and (b) $k_B T = 100 \text{ keV}$ plasmas. Contrary to the case of electrons, the peak value of the distribution becomes smaller as the initial temperature increases [The peak values are $p_x \simeq 140 m_e c$ in Fig. 5(a) and $p_x \simeq 170 m_e c$ in Fig. 5(b), respectively]. The front ions are accelerated only by the electrostatic field of the charge separation. The energy gain of the front ions tends to be large when the plasma temperature is low since the electric field becomes small

as the temperature increases.

In summary, we have examined charge separation effects in expanding electron-ion plasmas in the context of the diamagnetic relativistic pulse accelerator (DRPA). When the magnetized electron-ion plasma expands into a vacuum with no external magnetic field, only the surface electrons are efficiently accelerated by the DRPA. Because of the difference of the mobility between electrons and ions, charge separation occurs and generates a strong electrostatic field. This electric field accelerates the front ions and decelerates some of the front electrons. The initial plasma temperature affects the charge separation effect. As the temperature increases, the electric field caused by the charge separation becomes small. Therefore, electrons in high temperature plasmas are energized by the DRPA more efficiently compared to electrons in

low temperature plasmas. On the contrary, ions are energized by charge separation more efficiently in the low temperature case.

Acknowledgments

The work of KN and SPG was performed under the auspices of the U. S. Department of Energy (DOE) and was supported by the DOE Office of Basic Energy Sciences, Division of Engineering and Geosciences, the LDRD Program at Los Alamos, and the Sun-Earth Connections Theory Program of NASA. EL was supported by NASA Grant NAG5-7980 and LLNL Contract B510243.

-
- [1] J. Denavit, Phys. Fluids **22**, 1384 (1979).
 - [2] P. Mora, Phys. Rev. Lett. **90**, 185002 (2003).
 - [3] S. Okada, K. Sato, and T. Sekiguchi, Jpn. J. Appl. Phys., **20**, 157 (1981).
 - [4] B. H. Ripin, E. A. McLean, C. K. Manka, C. Pawley, J. A. Stamper, T. A. Peyser, A. N. Mostovych, J. Grun, A. B. Hassam, and J. Huba, Phys. Rev. Lett. **59**, 2299 (1987).
 - [5] R. D. Sydora, J. S. Wagner, L. C. Lee, E. M. Wescott, and T. Tajima, Phys. Fluids **26**, 2986 (1983).
 - [6] D. Winske, J. Geophys. Res. **93**, 2539 (1988).
 - [7] A. G. Sgro, S. P. Gary, and D. S. Lemons, Phys. Fluids **B1**, 1890 (1989).
 - [8] W. Peter and N. Rostoker, Phys. Fluids **25**, 730 (1982).
 - [9] E. Liang, K. Nishimura, H. Li, and S. P. Gary, Phys. Rev. Lett. **90**, 085001 (2003).
 - [10] E. Liang and K. Nishimura, “*Repeated bifurcation of relativistic magnetic pulse and cosmic gamma-ray bursts*,” (submitted to Phys. Rev. Lett.).
 - [11] K. Nishimura, S. P. Gary, H. Li, and S. A. Colgate, Phys. Plasmas **10**, 347 (2003).
 - [12] B. Marder, J. Comp. Phys. **68**, 48 (1987); D. E. Nielsen and A. T. Drobot, *ibid.* **89**, 31 (1990); A. B. Langdon, Comp. Phys. Comm. **70**, 447 (1992).